

THE EXPERIMENTAL CHARACTERIZATION OF LOCAL FRACTURE PROPERTIES

O. Kolednik, I. Sabirov, K. Unterweger
Erich Schmid Institute of Materials Science, Austrian Academy of Sciences, A-8700 Leoben, Austria

ABSTRACT

The paper describes modern experimental techniques which have been developed recently to measure local fracture properties. The techniques comprise quantitative fracture surface analysis and in-situ loading experiments, both in combination with digital image analysis. Examples are presented, such as the measurement of the local fracture initiation toughness, the determination of the local conditions for void initiation, the evaluation of the separation energy for cohesive zone modeling, and it is shown how in-situ loading experiments can be used to record the damage evolution in inhomogeneous materials.

1 INTRODUCTION

For the characterization of the fracture initiation toughness and the crack growth toughness of materials, fracture mechanics experiments are conducted. A problem is, however, that these values are not material constants, not even for homogeneous materials, but depend on the local constraint conditions. For example, the decreasing stress triaxiality near a free surface causes an increase of the local fracture toughness. Only the knowledge of the distribution of the local fracture toughness values along the crack front leads to the explanation of the well-known geometry and size effect of the crack growth resistance.

The problem is even larger, if inhomogeneous materials are considered, as the different phases in the material will exhibit different local fracture initiation toughness and crack growth toughness, each depending again on the constraint conditions. To understand the fracture properties of inhomogeneous materials, i.e., to learn how the microstructure influences the fracture properties, the determination of local fracture properties will be inevitable.

The purpose of this paper is, therefore, to present experimental procedures which have been developed recently in our research group to measure local fracture properties.

2 QUANTITATIVE FRACTURE SURFACE ANALYSIS

The main idea in all these procedures has been that it is possible to deduce local fracture properties from the shape of the fracture surfaces [1-3]. To do so, in most cases corresponding regions on both fracture surfaces of a broken specimen must be quantitatively analyzed. Nowadays, an automatic fracture surface analysis system is used for the quantitative fracture surface analysis [4,5]. The key part of this system is a matching algorithm which is able to find automatically homologue points in a stereo image pair which is taken in a scanning electron microscope (SEM). Homologue points are points in the two images which belong to the same physical point on the specimen. The stereo image pair is produced by tilting the specimen in the SEM. Standard SEM images with 1024 x 768 pixels at 256 gray levels yield 20000 to 30000 homologue points; extended images, which contain 4000 x 3200 pixels, yield up to 500000 homologue points.

From the homologue points and the three image parameters, magnification, working distance, and tilt angle, a three-dimensional model of the depicted fracture surface region is generated, called "digital elevation model", DEM. The DEM can be further processed to extract fracture surface profiles, profile and surface roughness parameters, and the fractal dimensions [6].

The application of the automatic fracture surface analysis system for the determination of the local fracture properties is described in the following section.

3 DETERMINATION OF LOCAL FRACTURE TOUGHNESS PARAMETERS

3.1 Local fracture initiation toughness

By analyzing corresponding regions on both halves of a broken fracture mechanics specimen and extracting profiles perpendicular to the pre-fatigue crack front, the critical crack tip opening displacement, COD_i , and the crack tip opening angle, $CTOA$, can be measured [7,8]. COD_i measures the local fracture initiation toughness at a given position, z , along the crack front, and $CTOA$ gives the local crack growth toughness. Figure 1a shows, as an example, two corresponding fracture surface profiles which are arranged so that the moment of fracture initiation is depicted: the ligament between the first void in front of the tip and the blunted pre-crack is just failing. The material is a cast metal matrix composite (MMC) with an under-aged Al6061 matrix and 10% Al_2O_3 particles with an average size of 10 μm .

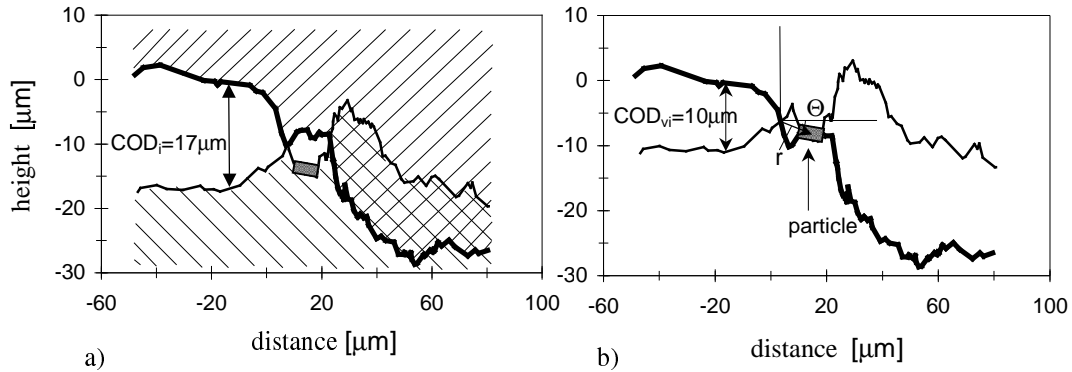


Figure 1: Crack profile through a particle in an MMC, (a) in the moment of fracture initiation, (b) in the moment of void initiation at the particle location.

3.2 Comparison between local and global fracture initiation toughness

The COD_i -values can be transformed to local values of the J-integral at fracture initiation, J_i , using the relationship,

$$J = m \sigma_y COD , \quad (1)$$

where σ_y is the yield strength and m a factor depending mainly on the strain hardening exponent [9]. Figure 2 compares the scattering values of the local J_i -values in the midsection region of a specimen to the global J_i -value from the fracture mechanics tests, where the crack extension was measured using the direct current potential drop technique. The data of three materials are given, (1.) a structural steel St37, (2.) a powder-metallurgically produced under-aged Al6061-MMC with 10% SiC particles with an average size of 100 μm , and (3.) the cast under-aged Al6061-MMC with 10% Al_2O_3 particles of Figure 1. For the St37 and the cast MMC, the global J_i -values correlate quite well with the average value of the local J_i -values. The standard deviation of the local J_i -values is much lower in the tougher St37 than in the MMC. For the powder-metallurgy

MMC, the global J_I -value correlates with the lower-bound value of the local J_I -values. This can be explained when it is assumed that in this material the fracture of a single particle at low COD may cause the fracture neighboring particles within a certain region in the specimen. This region is so large that fracture initiation is detected by the potential drop technique. Then the crack extension stops and the next local crack extension step occurs at a higher COD. For the St37 and the cast MMC, the local crack extension steps at low COD are so small that they are not detected by the potential drop technique.

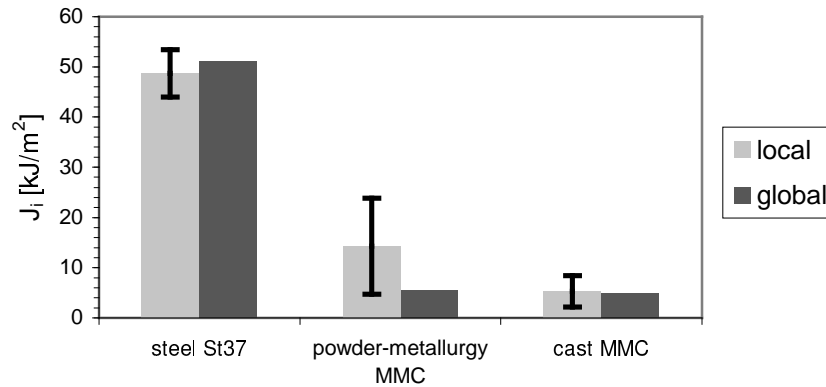


Figure 2: Comparison between the local and global fracture initiation toughness values.

3.3 Local conditions for void initiation

If the lower profile of Figure 1a is shifted vertically so that the two profiles touch each other at the location of the particle, we get a sketch of the crack at the moment of void initiation (Figure 1b), and the crack tip opening displacement at the moment of void initiation, COD_{vi} , can be measured. This value, COD_{vi} , or the transformed value, J_{vi} , gives the resistance of the material against void initiation and, thus, it can be considered as a measure of the local “void initiation toughness” [10].

The COD_{vi} -values and the polar coordinates (r, θ) of the particle location with respect to the crack tip can be used to estimate the maximum particle stress at the moment of void initiation [11]: For individual particles, the mesoscopic stress tensor acting on the particle location is evaluated from J_{vi} by means of the HRR-field theory. Subsequently, a non-linear Mori-Tanaka type mean-field approach is employed to determine the maximum principal particle stress, σ_{max}^p . Hereby, it does not matter whether void initiation occurs by particle fracture or particle/matrix decohesion. It has been shown in [11] that this procedure can be applied not only for MMCs but also for particles in other engineering materials. For example, it is seen in Figure 3 that the fracture behavior of the steel St37 is mainly influenced by the distribution of the MnS inclusions. Voids are initiated by decohesion at maximum stresses in the MnS-inclusions ranging between 960 MPa and 1480 MPa. The values increase with decreasing inclusion diameter.

3.4 Evaluation of the separation energy

For micro-ductile fracture, the separation energy, I , represents the plastic work per unit area required for the formation of the dimple structures on the two fracture surfaces. Stüwe [1,2], introduced a model to estimate the specific plastic strain energy to form the two dimpled fracture surfaces of a micro-ductile crack based on a model of void growth, R_{surf} . The result is

$$R_{surf} = 2S\bar{\sigma}h_0, \quad (2)$$

where $\bar{\sigma}$ is an appropriate mean flow stress of the material, which can be estimated by

$$\bar{\sigma} = \sigma_u \frac{\exp(n)}{(1+n)n^n}. \quad (3)$$

σ_u is the ultimate tensile strength, n the strain hardening coefficient, and S denotes a shape factor of the dimples which has been found to be approximately $S \approx 0.25$ [2]. In Eqn 2, h_0 is a characteristic dimple height which can be determined from the topography of the corresponding fracture surface regions on both specimen halves [3].

A typical view of the fracture surface of a structural steel, St37, is shown in Figure 3. A crack profile, obtained from the corresponding regions on both halves of the specimen, is presented on the right hand side. A characteristic misfit of $2h_0 \approx 80 \mu\text{m}$ is measured. This, inserted into Eqn 2 for $\bar{\sigma} \approx 600 \text{ MPa}$, gives a value of $R_{surf} \approx 12 \text{ kJ/m}^2$. Adding a reasonable estimate for the specific energy for void initiation ($R_{vi} \approx 2 \text{ kJ/m}^2$) to R_{surf} , we arrive at an estimate for the separation energy, $\Gamma = R_{surf} + R_{vi} \approx 14 \text{ kJ/m}^2$.

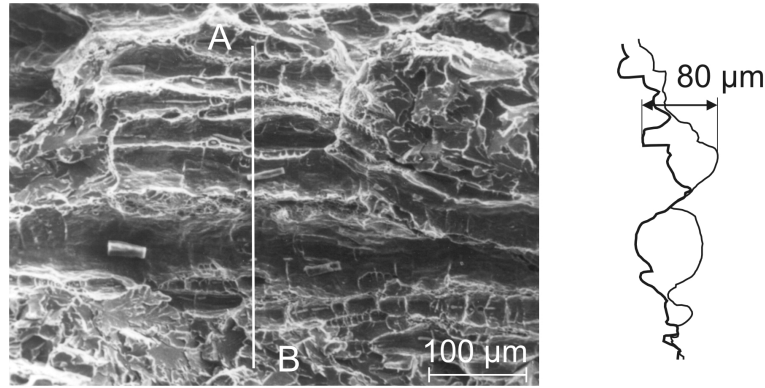


Figure 3: Fracture surface region of the steel St37 with crack profile.

3.5 In-situ deformation experiments

Instead of analyzing stereo image pairs, our digital image analysis system can be also used to find homologue points in micrographs that are taken at different loading stages during an in-situ loading experiment in the SEM. The homologue points form a displacement field that can be numerically derived to evaluate maps of the in-plane strains. The method was first introduced by Davidson as “stereomaging technique” [12]. We apply a new analysis system that provides high accuracy and lateral resolution [13].

An example of such an analysis is presented in Figure 4, for a powder-metallurgy MMC with $100 \mu\text{m}$ large SiC particles, see [14] for details. Figure 4a,b shows the region around Particle 3 at the deformation stages before and after particle fracture, at 0.56 and 1.10% global tensile strain. The corresponding maps of the local tensile strains are given in Figure 4c,d. At 0.56% global strain, the local strains below Particle 3 are very low. Strong deformation occurs in the area around the pre-damaged Particle 4, which was completely fractured already before the loading began. After the fracture of Particle 3, a strong deformation band develops below Particle 2. This

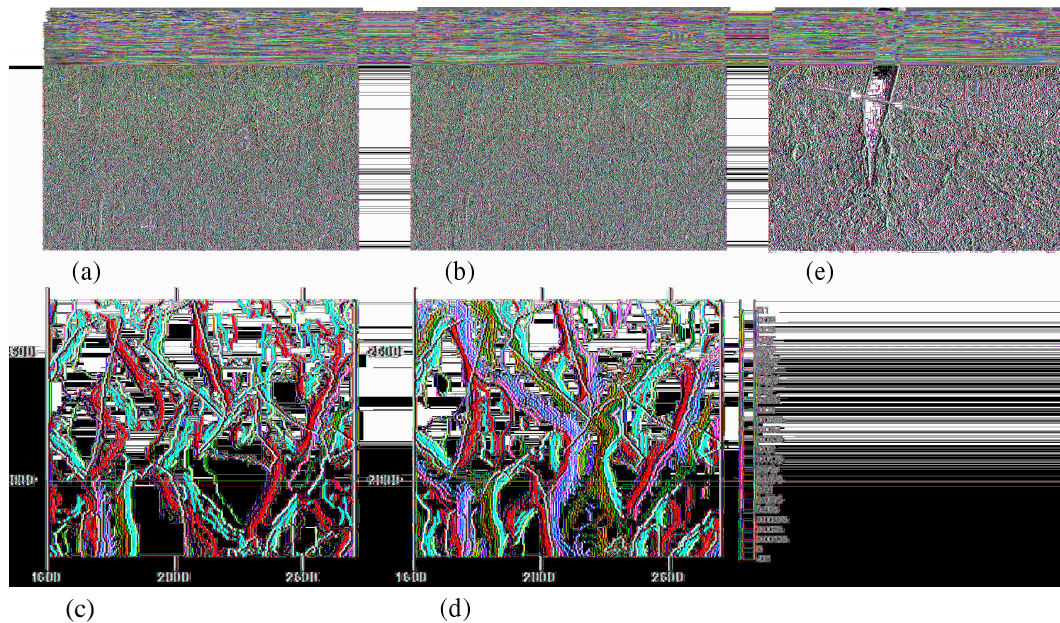


Figure 4: SEM-micrographs of an-situ deformation experiment (upper row) with maps of the tensile strains 0.56 and 1.10% global strain.

deformation band causes the fracture at the upper corner of Particle 1. The average strain in the deformation band reaches about (3-4)%. Final fracture of the specimen occurs at 2.3% global strain.

In this material, the deformation behavior is mainly determined by the development of particle damage. Local plastic deformation starts at pre-damage sites. First shear bands connect these failure sites. With increasing load, new deformation bands develop in the matrix, mostly orientated 45° to the loading axis. Further loading leads to new particle failure sites, which themselves lead to increased matrix deformation. Cracks are initiated by the fracture of particles which occurs at different stress levels; some particles have been already fractured during the processing of the material. The critical event concerning the fracture resistance is the extension of the particle cracks into the matrix material. The sparse data available up to now suggests that this might occur at a critical COD of about $6 \mu\text{m}$, see Figure 4e.

4 SUMMARY

Quantitative fracture surface analysis and in-situ loading experiments, both in combination with modern digital image analysis, allows the determination of local fracture properties. Some examples have been presented in this paper. The knowledge of local fracture toughness parameters is important for understanding of the deformation and fracture behavior of inhomogeneous materials. For the numerical simulation of crack growth in engineering materials and structural components, such data are valuable, as parameters can be deduced to control the crack growth in the numerical analysis. A classical example is the local crack tip opening angle which can be assumed to be constant during the crack extension, after an initial transition region [15,16]. The estimate of the separation energy is useful for the application of the cohesive zone model [17,18]. A still unsolved problem is the characterization of the local conditions for crack initiation.

ACKNOWLEDGEMENTS

The authors acknowledge gratefully the financial support of this work by the Fonds zu Förderung der wissenschaftlichen Forschung under the project number P14333-N02.

REFERENCES

1. Stüwe, H.P., The work necessary to form a ductile fracture surface. *Engineering Fracture Mechanics* 13, 231-236, 1980.
2. Stüwe, H.P., The plastic work spent in ductile fracture. *Three-dimensional Constitutive Relations and Ductile Fracture*, S. Nemat-Nasser, Ed., North-Holland, Amsterdam, 213-221, 1981.
3. Kolednik, O., Stüwe, H.P., Abschätzung der Reißfähigkeit eines duktilen Werkstoffes aus der Gestalt der Bruchfläche. *Zeitschrift für Metallkunde* 73, 1982, 219-223, 1982.
4. Stampfl, J., Scherer, S., Gruber, M., Kolednik, O., Reconstruction of surface topographies by scanning electron microscopy for application in fracture research. *Applied Physics A63*, 341-346, 1996.
5. Scherer, S., Kolednik, O., A New system for automatic surface analysis in SEM. *Microscopy and Analysis* 70, 15-17, 2001.
6. O. Kolednik, P. Schwarzböck, *Fracture Mechanics: Applications and Challenges, Proc. of ECF13*. M. Fuentes, M. Elices, Eds., Paper 1U.60, Elsevier, Amsterdam, 2000.
7. Kolednik, O., Stüwe, H.P., The stereophotogrammetric determination of the critical crack tip opening displacement. *Engineering Fracture Mechanics* 21, 145-155, 1985.
8. Stampfl, J., Scherer, S., Berchthaler, M., Gruber, M., Kolednik, O., Determination of the fracture toughness by automatic image processing. *International Journal of Fracture*, 78, 35-44, 1996.
9. Shih, C.F., Relationship between the J-integral and the crack tip opening displacement for stationary and extending cracks. *Journal of the Mechanics and Physics of Solids* 29, 305-326, 1981.
10. Qiu, H., Enoki, M., Kawaguchi, Y., Kishi, T., A model for the static fracture toughness of ductile structural steel. *Engineering Fracture Mechanics* 70, 599-609, 2003.
11. Sabirov, I., Duschlbauer, D., Pettermann, H.E., Kolednik, O., The determination of the local conditions for void initiation in front of a crack tip for materials with second-phase particles. *Materials Science and Engineering*, submitted.
12. Davidson, D.L., The observation and measurement of displacement and strain by stereomaging. *Scanning Electron Microscopy* 11, 79-81, 1979.
13. Tatschl, A., Kolednik, O., A new tool for the experimental characterization of microplasticity. *Materials Science and Engineering A339*, 2003, 265-280.
14. Unterweger, K., Kolednik, O., Pippan, R., The experimental determination of the local deformation and damage behavior of MMCs. *Proceedings of the Fourteenth International Conference on Composite Materials, ICCM-14*, Paper ID 1029. Society of Manufacturing Engineers, Dearborn, Michigan, USA, 2003.
15. J.C. Newman Jr., An elastic-plastic finite element analysis of crack initiation, stable crack growth, and instability. *ASTM STP* 833 (1984) 93-117.
16. W.-Y. Yan, G.X. Shan, O. Kolednik, F.D. Fischer, A numerical simulation of the crack growth in a smooth CT specimen. *Key Engineering Materials* 145-149 (1998) 179-184.
17. Needleman, A., A continuum model for void nucleation by inclusion debonding. *Journal of Applied Mechanics* 54, 525-531, 1987.
18. Chen, C.R., Kolednik, O., Scheider, I., Siegmund, T., Tatschl, A., Fischer, F.D., On the determination of the cohesive zone parameters for the modeling of micro-ductile crack growth in thick specimens, *International Journal of Fracture*, 120, 517-536, 2003.